Carbohydrate Polymers 113 (2014) 490–499

Contents lists available at ScienceDirect

Carbohydrate Polymers

journal homepage: www.elsevier.com/locate/carbpol

Influence of grape pomace extract incorporation on chitosan films properties

Andreia S. Ferreira [a], Cláudia Nunes [a,*], Alichandra Castro [b], Paula Ferreira [b], Manuel A. Coimbra [a]

[a] QOPNA, Departamento de Química, Universidade de Aveiro, 3810-193 Aveiro, Portugal
[b] CICECO, Departamento de Engenharia de Materiais e Cerâmica, 3810-193 Aveiro, Portugal

ARTICLE INFO

Article history:
Received 2 April 2014
Received in revised form 8 July 2014
Accepted 9 July 2014
Available online 22 July 2014

Keywords:
Solubility
Atomic force microscopy
Mechanical properties
Antioxidant activity
Edible films

ABSTRACT

Chitosan has been studied as a renewable polymer to form edible films allowing the incorporation of functional compounds. The aim of this work was to evaluate the effects in the chitosan films properties of the incorporation of grape pomace extracts: 0.15% of hot water extract (mainly polysaccharides), 0.15 and 0.3% of chloroform extract (wax), and 0.3 and 0.75% of *n*-hexane extract (oil). The evaluation of the surface morphology revealed that the films with the aqueous extract had the most homogeneous and smoother topography. The incorporation of higher proportion of wax and oil led to changes in mechanical properties of the films, namely lower resistance and stiffness. The chitosan-based films with 0.75% oil demonstrated a 75% decrease of solubility in water, due to their hydrophobicity, as confirmed by the contact angle and surface free energy measurements. The hydrophobic films showed higher antioxidant capacity in organic medium (ABTS and DPPH assays) whereas the most hydrophilic films showed an improvement in FRAP and reducing power assays. Therefore, all the chitosan-based films prepared by incorporation of these grape pomace extracts are promising for food shelf life extension.

1. Introduction

The use of edible films and coatings to improve the shelf life of food products from renewable biopolymers has been increasing, offering advantages over synthetic materials due to their biodegradability (Tharanathan, 2003). Chitosan, the linear cationic (1 → 4)-2-amino-2-deoxy-β-D-glucan produced from chitin by partial deacetylation, is being studied extensively owing to its biocompatibility, biodegradability, and absence of toxicity (Busilacchi, Gigante, Mattioli-Belmonte, Manzotti, & Muzzarelli, 2013). This polysaccharide is filmogenic and yields stable films with a particular adhesiveness towards biological surfaces because of its positive charge at neutral/acidic pH (Aranaz et al., 2009; Kumar, Muzzarelli, Muzzarelli, Sashiwa, & Domb, 2004). Chitosan, mainly chitooligomers, has shown a significant scavenging capacity against different radical species, being the results comparable to those obtained for commercial antioxidants, such as Trolox (6-hydroxy-2,5,7,8-tetramethylchroman-2-carboxylic acid) (Aranaz et al., 2009; Chen et al., 2003). In addition, chitosan has the ability to chelate metal ions involved in catalysis of oxidative reactions. These properties allow extending the food shelf life, since oxidation is a problem affecting food quality and biological applications (Chien, Sheu, Huang, & Su, 2007). Besides, it has been reported intrinsic antimicrobial activity in chitosan films, inhibiting the growth of a wide variety of bacteria and fungi, avoiding food spoilage (Dutta, Tripathi, Mehrotra, & Dutta, 2009; Kong, Chen, Xing, & Park, 2010).

Therefore, chitosan is a suitable material for food packaging film or coating usages. Nevertheless, pure chitosan films are fragile and need plasticisers, such as glycerol, to reduce frictional forces between the polymer chains, thus improving mechanical properties (Bourbon et al., 2011; Srinivasa, Ramesh, & Tharanathan, 2007). Furthermore, the incorporation of other antimicrobial and/or antioxidant compounds of natural origin into chitosan films is a feasible way to enhance chitosan films' functional properties, enlarging their potential applications. A great number of works report the influence and the behaviour of bioactive compounds on chitosan films such as essential oils (Hosseini, Razavi, & Mousavi, 2009; Moradi et al., 2012; Sánchez-González, Cháfer, Chiralt, & González-Martínez, 2010a; Sánchez-González, González-Martínez, Chiralt, & Cháfer, 2010b) or phenolic compounds (Rubilar et al., 2013; Siripatrawan & Harte, 2010).

Grapes are the second world's largest fruit crop. About 80% of the total crop is used in winemaking and pomace represents

* Corresponding author. Tel.: +351 234 370706; fax: +351 234 370084.
E-mail address: claudianunes@ua.pt (C. Nunes).

http://dx.doi.org/10.1016/j.carbpol.2014.07.032
0144-8617/

approximately 20% of the weight of grapes processed. Grape pomace, consisting of skins, seeds, and stems, is a rich source of phenolic compounds, lipids, waxes, polysaccharides, and proteins. Since grape pomace is an abundant by-product, its valorisation has a large economic interest (Deng, Penner, & Zhao, 2011; Schieber, Stintzing, & Carle, 2001). The preparation of films by the incorporation of grape pomace extracts into different commercial polysaccharide matrices, such as low methoxyl pectin, sodium alginate, and Ticafilm, has been already proposed (Deng & Zhao, 2011). However, the addition of grape pomace extracts into chitosan-based films has not yet been reported in literature.

The purpose of this work consists to prepare chitosan-based films for food applications with improved possibility of modulation their properties by incorporation of three different grape pomace extracts, namely the water soluble compounds, the grape skin wax, and the grape seed oil. The influence of these extracts on the physico-chemical, mechanical, antioxidant, and antimicrobial properties of the films, was evaluated.

2. Material and methods

2.1. Samples and reagents

Grape pomace extract (*Vitis vinifera*, var. Touriga Nacional), a by-product from winemaking, was provided by Dão Sul S.A. (Portuguese winemaking company, Carregal do Sal, Portugal) in 2011. The grape pomace was stored at −18 °C until use (6 months). Chitosan of medium molecular weight with 85% of deacetylation and 2,2-diphenyl-1-picrylhydrazyl (DPPH) were supplied by Sigma-Aldrich (St. Louis, MO, USA), glycerol (99.5%) was purchased from Sigma-Aldrich (Milwaukee, USA), and 2,2′-azinobis-(3-ethylbenzothiazoline-6-sulfonic acid (ABTS, 99%) was purchased from Fluka (St. Louis, MO, USA). Other reagents were of analytical grade or higher available purity.

2.2. Grape pomace extracts

2.2.1. Aqueous extraction

The hot water extract was obtained according to the method described by Deng and Zhao (2011), with some modifications. The skins were manually separated from the stems and seeds and dried at 40 °C for 48 h. The dried skins were milled to pass a 0.75 mm mesh (ZM 1000, Resh). Distilled water, preheated at 70 °C, was added to the pomace powder at a ratio of 1:10 (w/v) and the mixture was stirred at 4000 rpm for 10 min for enhancing the release of the soluble compounds into the solution. The mixture was placed into a 50 °C water bath for 45 min following by centrifugation (Sigma, Laboratory Centrifuges 3k30) at 15,000 rpm during 20 min at 4 °C (this procedure was performed 3 times). The obtained solution was filtered under vacuum through ashless paper filters, dialysed (12–14 kDa) and freeze-dried. The extraction yield was 0.9% (w/w) and the extract was composed by 72.5% of polysaccharides, measured by the alditol acetates of neutral sugars (Coimbra, Waldron, & Selvendran, 1994) and *m*-phenylphenol reagent for uronic acids (Blumenkrantz & Asboe-Hansen, 1973), 21.5% of proteins, measured by the bicinchoninic acid assay (Krohn, 2001), and 5.7% of polyphenols, determined by the Folin–Ciocalteu reagent (Ainsworth & Gillespie, 2007).

2.2.2. Waxes extraction

The residue obtained from the aqueous extraction (Section 2.2.1) was used to obtain the wax rich extract. The residue was dried at 40 °C for 18 h and afterwards was homogenised with chloroform, at a ratio of 1:10 (w/v), in a Pyrex glass bottle. The closed bottle was placed into a 70 °C bath for 30 min. Then, the mixture was filtered and the solvent evaporated under reduced pressure. The extraction yield was 6.5% and the presence of waxes was confirmed by the FT-IR bands ranging between 3600 and 3200 cm^{-1}, 2916 and 2848 cm^{-1}, and 1736 and 1690 cm^{-1}, which are characteristic of the triacylglycerides (see Supplementary material Fig. S1).

Table 1
Composition of the prepared chitosan-based films.

Films*	Grape pomace extract	% Chitosan (w/v)	% Grape pomace extract (w/v)
Ch	–	1.5	–
HWE	Hot water extract	1.5	0.15
W1	Grape skin wax	1.5	0.15
W2		1.5	0.3
Oil1	Grape seed oil	1.5	0.3
Oil2		1.5	0.75

* Ch—Chitosan film (control); HWE—Chitosan film with hot water extract; W—Chitosan film with wax; Oil—Chitosan film with oil.

2.2.3. Oil extraction

The seeds were washed, dried at 40 °C for 18 h, and milled to pass a 0.5 mm mesh (ZM 1000, Resh). The powdered seeds were extracted in a 200 mL Soxhlet extractor with 150 mL of *n*-hexane at 60 °C for 5 h. After extraction, the solvent was evaporated under reduced pressure. The extraction yield was 16.7% and the fatty acid composition was 70% of linoleic acid, 18% of oleic acid, 7% of palmitic acid, and 5% of stearic acid, analysed by gas chromatography (Perkin Elmer Clarus 400) (Aued-Pimentel, Lago, Chaves, & Kumagai, 2004).

2.3. Chitosan-based films preparation

Six chitosan solutions of 1.5% (w/v) were prepared by dissolving the chitosan in 5% (v/v) aqueous acetic acid solution with stirring at room temperature for 18 h. The different grape pomace extracts were added to each one of the chitosan solutions in the proportions given in Table 1. These were the optimised proportions for each extract concerning the parameters understudy, namely the higher antioxidant activities and lower solubility in aqueous media. The chitosan solutions were homogenised for 30 min with continuous stirring. Afterwards, glycerol was added at 0.5 mL/g, as plasticiser. This mixture was placed in a water bath at 50 °C with stirring for 10 min for homogenisation. After cooling to room temperature, the solutions were filtered under vacuum through a sintered glass filter (porosity G2, 40–90 μm) and degassed. This solution (31 g) was transferred into a plexiglass plate with 144 cm^2 and 3 mm deep. The plates were placed in an oven for 18 h at 35 °C for film formation by solvent casting. A control film was also prepared only with chitosan, no extracts added. Table 1 summarises the composition of the chitosan-based films prepared.

2.4. Chitosan-based films characterization

2.4.1. FT-IR

The FT-IR spectra of the films were obtained using a Golden Gate single reflection diamond ATR system in a Perkin Elmer Spectrum BX spectrometer. Spectra were recorded at the absorbance mode from 4000 to 500 cm^{-1} (mid-infrared region) at a resolution of 16 cm^{-1}. Five replicates (64 co-added scans) were collected for each sample.

2.4.2. Solubility in aqueous medium

The films solubility was determined in water at pH 6.5 according the method described by Nunes et al. (2013). Briefly, one square (4 cm^2) of film was placed in 30 mL of distilled water for 7 days. The solubility was determined by the percentage of weight loss of the film (105 °C, 16 h), on a dry weigh basis, after being immersed in

distilled water. The analysis was performed in triplicate by using three times a square of film obtained from each film-forming solution.

2.4.3. Wettability and surface free energy

The measure of the static water contact angle on the surface (wettability) of chitosan-based films was performed using a contact angle measuring system (OCA 20, Dataphysics) at room temperature. A sessile drop of 3 μL of ultrapure water was dispensed on the surface of each film (1 × 10 cm) using a microsyringe.

The surface free energy, dispersive phase, and polar phase were determined based on the contact angle measurements of three different standard liquids: ultrapure water (3 μL), formamide (1.5 μL), and diiodomethane (1.5 μL), at room temperature, using Owens-Wendt-Rabel and Kaelble (OWRK) method. The contact angles of the drops were calculated by an image analysis software (SCA20 M4 Dataphysics) using the Laplace–Young method (Nunes et al., 2013). Nine droplet images were obtained for each film surface.

2.4.4. Surface morphology by atomic force microscopy

Atomic force microscopy (AFM) analyses of the samples were performed under ambient conditions using a multimode Nanoscope III microscope, Digital Instruments, operating in tapping mode. Silicon AFM tips (TAP300 BudgetSensors) with a resonance frequency of 300 kHz and a force constant of 40 N/m were used. The scan rate varied from 1–2 Hz and the tip artifacts were excluded by using fresh tips. The program used to obtain the two-dimensional (2D) images and the height profiles of the chitosan-based films was the WSxM 4.0 Develop 12.0 (Nanotec Electronica S.L., 2008) and the program used to obtain the three-dimensional (3D) images was the Surfer Version 8.00 (Golden Software Inc. 2002). The fibre diameters, height profile, and roughness medium square were calculated using the WSxM 4.0 Develop 12.0 program. The maximum values of the height were calculated by averaging the maximum values of at least 8 profile patterns traced along each 2D topographic image.

2.4.5. Mechanical properties

The mechanical properties of films were evaluated as described by Nunes et al. (2013). The films were stored under controlled conditions of moisture (45% humidity) and temperature (22 °C), and protected from light during 4 months before analysis. The tensile test was performed at room temperature using a texture analyser equipment (model TA.Hdi, Stable Micro Systems) equipped with fixed grips lined with thin rubber on the ends. All films were cut in strips with 90 mm length and 10 mm wide for the determination of tensile properties. The film ends were mounted on the grips and the initial grip separation was set at 50 mm. The crosshead speed was set at a constant rate of 0.5 mm/s. Young's modulus (YM), percentage elongation or strain at break (E), and tensile strength or stress at break (TS) were determined from stress–strain curves obtained from uniaxial tensile tests to film failure. These parameters were calculated based on ASTM D 882-83 standard method. At least five samples of each film type were tested. Film thickness (0.039–0.057 mm) was measured to the nearest 0.001 mm using a hand-held micrometer (Mitutoyo Corporation), along the length of the rectangular strip.

2.4.6. Antioxidant activity

2.4.6.1. ABTS assay. The antioxidant activity of the films produced was determined by an adaptation of the method of 2,2′-azinobis-(3-ethylbenzothiazoline-6-sulfonic acid, ABTS, as described by Nunes et al. (2013). Briefly, a solution of 7 mM ABTS was prepared in 2.45 mM potassium persulfate. This solution was left in the dark, at room temperature, for 12–16 h for $ABTS^{\bullet+}$ formation. One square (1 cm^2) of film was placed in 3 mL of $ABTS^{\bullet+}$ solution (diluted 1:80 in ethanol) and left to react in the dark with orbital stirring at 80 rpm. The absorbance at 734 nm (Jenway 6405 UV/vis) of the solution was measured 6 h later. All measurements were performed in triplicate.

2.4.6.2. DPPH assay. The antioxidant activity of the films was also determined by an adaptation of the method of 2,2-diphenyl-1-picrylhydrazyl (DPPH), described by Huang, Ou, and Prior (2005). The DPPH (1.25 mg) was dissolved in 50 mL of ethanol and the concentration of the solution was adjusted to obtain an absorbance value between 0.700 and 0.800 at 517 nm using a spectrophotometer (Jenway 6405 UV/vis). One square (1 cm^2) of film was placed in 3 mL of DPPH solution and left to react in the dark with orbital stirring at 80 rpm. The absorbance of the solution at 517 nm was measured after 68 h, as well as, the absorbance of the DPPH solution without film (blank). All measurements were performed in triplicate. The antioxidant activity was determined by the percentage of inhibition of the DPPH.

2.4.6.3. FRAP assay. The Ferric Reducing Antioxidant Power (FRAP) method was performed according to Benzie and Strain (1996). A ferric salt, $Fe(III)(TPTZ)_2Cl_3$ (TPTZ—2,4,6-tripyridyl-*s*-triazine), was used as oxidant. A FRAP unit was defined, arbitrary, as a reduction of 1 mol of Fe(III) to Fe(II). A solution of $FeCl_3$ (20 mM) was prepared in distilled water and the TPTZ was prepared in 40 mM HCl. To prepare the FRAP reagent, 2.5 mL of TPTZ were mixed with 2.5 mL $FeCl_3$, 25 mL acetate buffer (0.3 M, pH 3.6), and 3 mL of distilled water. A film with 0.25 cm^2 was placed in 3 mL of FRAP solution and the absorbance at 595 nm was measured 24 h later. The absorbance of the FRAP solution without film was also measured (blank). The antioxidant activity was determined subtracting the blank to the film absorbance. All measurements were performed in triplicate.

2.4.6.4. Reducing power assay. The reducing power of chitosan films was carried out according to Zhang, Yang, Tang, Hu, and Zou (2008). One square of film (1 cm^2) was incubated with 1 mL of 1% (w/v) potassium ferricyanide at 50 °C for 30 min. One mL of 10% (w/v) trichloroacetic acid was added to the mixture, which was then centrifuged at 5000 rpm for 5 min (Kubota, 2010). The upper layer of the solution (2 mL) was mixed with 1 mL of distilled water and 0.2 mL of 0.1% (w/v) $FeCl_3$ and the absorbance was measured at 700 nm. All measurements were performed in triplicate.

2.5. Statistical analyses

The results of solubility, wettability, mechanical properties, and antioxidant activity were statistically evaluated using F and t-Student tests of Microsoft Excel 2010, at a 95% significance level.

3. Results

3.1. FT-IR spectroscopy of chitosan films

The Fourier transform mid-infrared (FT-IR) spectra obtained in the wavelength range of 4000–500 cm^{-1} of the different chitosan-based films: control (Ch), 0.15% of aqueous extract (HWE), 0.15 and 0.3% of grape skin waxes (W1 and W2), and 0.3 and 0.75% of grape seed oil (Oil1 and Oil2) are shown in Fig. 1.

The chitosan shows a broad band ranging between 3600 and 3000 cm^{-1}, attributed to the O—H and N—H stretching vibration, a broad band between 3000 and 2800 cm^{-1} attributed to C—H stretching vibration, and peaks at 1642 cm^{-1}, 1556 cm^{-1}, and at 1320 cm^{-1} attributed to C=O stretching (amide I), N—H bending (amide II), and to C—N stretching (amide III), respectively (Leceta, Guerrero, Ibarburu, Dueñas, & de la Caba, 2013; Rubilar et al., 2013).

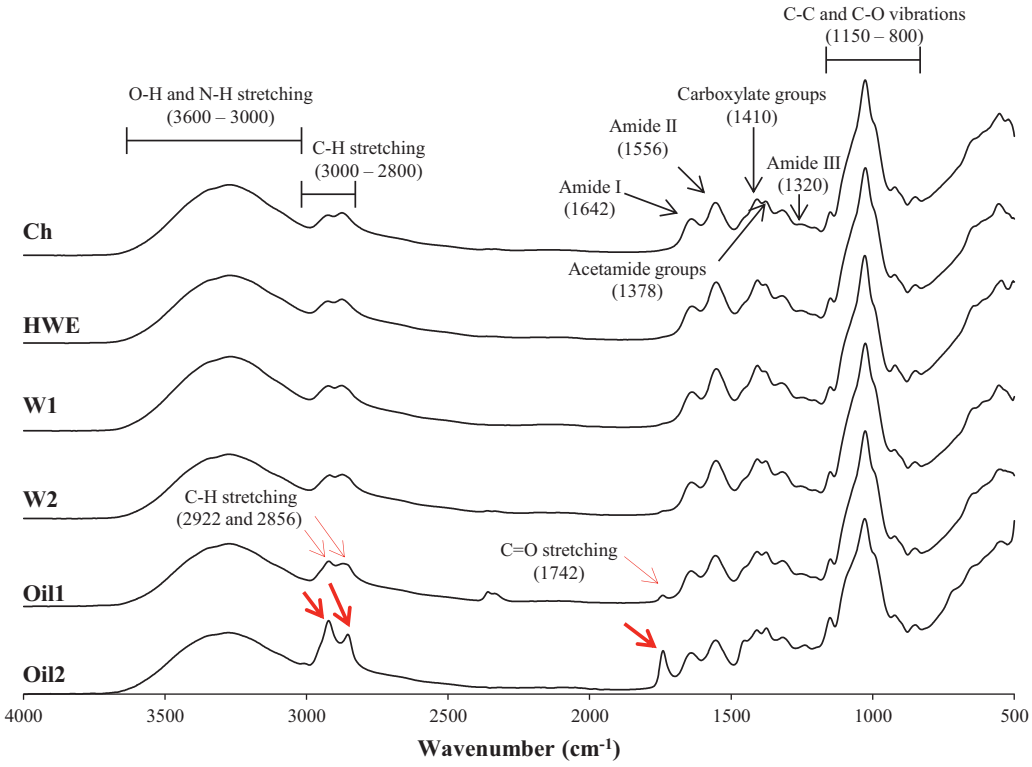

Fig. 1. FT-IR spectra of chitosan film (Ch) and chitosan-based films with 0.15% of aqueous extract (HWE), 0.15 and 0.3% of grape skin waxes (W1 and W2), and 0.3 and 0.75% of grape seed oil (Oil1 and Oil2).

The band that appears at 1378 cm^{-1} is assigned to the acetamide groups, which indicates that the chitosan was not totally desacetylated (85% deacetylation degree) according to the manufacturer. The bands in the range 1150–800 cm^{-1} correspond to the C—C and C—O linkages from the polysaccharide backbone and also from the presence of glycerol (Fernandes, 2010; Leceta et al., 2013). The absorption peak at 1410 cm^{-1} corresponds to the carboxylate groups due to the presence of residual acetic acid used for the preparation of the chitosan forming film solution (Lagaron, Fernandez-Saiz, & Ocio, 2007). In fact, the amount of acetic acid used (5% w/w) seemed to be higher than that required to dissolve chitosan. However, the presence of acetic acid in the film, although not quantitatively measured, does not promote the decrease of the pH when the films are immersed in aqueous solutions (data not shown). On the contrary, the pH increases, possibly due to the protonation of the glucosamine residues (Shahidi, Arachchi, & Jeon, 1999). In order to avoid the presence of acetic acid in the films, which could be inappropriate for some applications, other weak acids could be also used, such as formic and lactic acids (Soares, Mendes, & Vicente, 2013).

The spectra of HWE, W1, and W2 showed the same pattern as the Ch, with no visible change in the peak intensities and wavenumbers shift. As the incorporation of aqueous extract and waxes did not change the FT-IR spectra when compared with the chitosan film, it can be inferred that no relevant changes in covalent bonds and chemical interactions occurred. However, in the spectra of Oil1, and mainly in Oil2, the peaks at 2922 and 2856 cm^{-1}, related to the stretching symmetric and asymmetric vibration of C—H bonds in CH_2 and CH_3 groups, were more intense. Besides, a new peak appears at 1742 cm^{-1} due to carbonyl groups (C=O) stretching vibration of triacylglycerides, confirming the incorporation of the oil into the chitosan-based films. The analysis of FT-IR spectra allowed confirming the oil incorporation on the film matrix.

3.2. Solubility

Fig. 2 shows the weight loss obtained for the control film (Ch) and for the chitosan-based films enriched with aqueous extract obtained from grape pomace (HWE), waxes from grape skins (W1 and W2), and grape seed oil (Oil1 and Oil2).

The solubility of the chitosan films was significantly lower by the incorporation of the oil in a higher concentration (0.75%; Oil2) with only 8 wt% loss, resulting in films with 75% lower solubility when compared to the Ch films. This phenomenon is due to the hydrophobic nature of the oil present in the film, as proved in mid-infrared analysis (Fig. 1), also described when cinnamon or clove essential oils were incorporated into chitosan films (Hosseini et al., 2009; Ojagh, Rezaei, Razavi, & Hosseini, 2010). For all the others, the

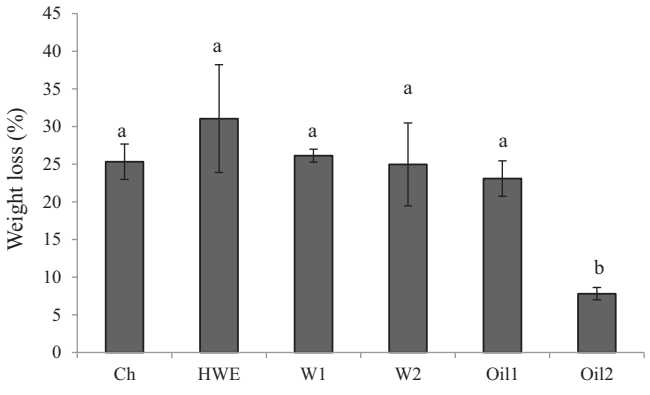

Fig. 2. Solubility (weight loss %) in distilled water (pH 6.5) of chitosan film (Ch) and chitosan-based films with 0.15% of aqueous extract (HWE), 0.15 and 0.3% of grape skin waxes (W1 and W2), and 0.3 and 0.75% of grape seed oil (Oil1 and Oil2) after 7 days with stirring. Different letters represent values that are significantly ($p < 0.05$) different ($n = 3$).

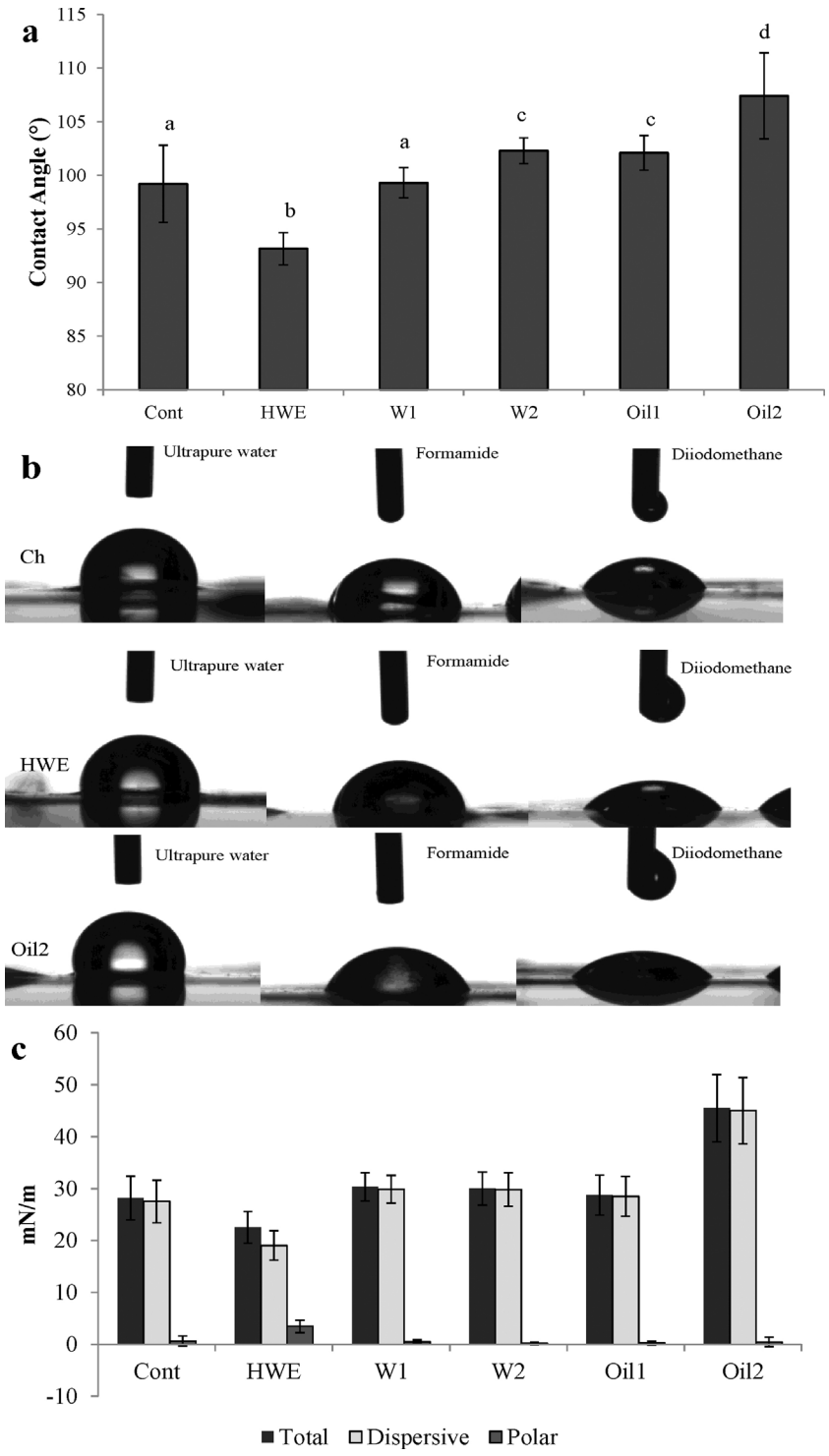

Fig. 3. Wettability and surface free energy analyses. (a) Contact angles of chitosan film (Ch) and chitosan-based films prepared according to Table 1. (b) Photographs of the interaction between the drop of ultrapure water (first column), formamide (second column), and diiodomethane (third column) and the Ch, HWE, and Oil2 films. (c) Surface free energy of the films. Different letters represent values that are significantly ($p < 0.05$) different ($n = 9$).

average solubility ranged between 23 and 31%. The higher solubility of these chitosan-based films is attributed to the water solubility of chitosan and glycerol at pH 6.5 (Ojagh et al., 2010).

The resistance of the chitosan films with 0.75% of oil (solubility <10%) in water could be important for applications where films with low solubility in water are required, such as packaging of highly moisture foods (Rhim, Weller, & Ham, 1998).

3.3. Wettability and surface free energy

Fig. 3a shows the effect of the incorporation of the different grape pomace extracts on the surface wettability of the chitosan-based films. When a drop of ultrapure water is placed on the film surface, the water drop does not spread, forming a spherical cap on the film surface with a specific contact angle (Fig. 3b, first column). This contact angle is a measure of the non-covalent forces between

the ultrapure water and the first monolayer (surface) of the films and is an indicator of their superficial hydrophilic/hydrophobic properties (Moradi et al., 2012; Nunes et al., 2013).

The ultrapure water contact angles ranged from 93.4 to 107.4° for all the films analysed, despite the hydrophilic nature of chitosan. These values are similar to those reported by Nunes et al. (2013) (101.4–105.5°) for chitosan films cross-linked with genipin and grafted with caffeic acid, allowing to infer that these films have an hydrophobic character. The HWE film, which showed the lowest value of contact angle (93.4° ± 1.5), was the most hydrophilic film in the set. The incorporation of the aqueous extract results in a more hydrophilic film. These results are in agreement with the surface wettability studies of chitosan-soy protein (Silva et al., 2007) and chitosan-grape seed extract (relatively high levels of flavonoids) films (Moradi et al., 2012). Oppositely, the addition of 0.3% of wax and oil and 0.75% of grape seed oil led to an increase of the film contact angle by 3% (W2 and Oil1), and 8% (Oil2), comparing with the control film. Similar behaviour was observed in films prepared with the incorporation of cinnamon essential oil (Ojagh et al., 2010), *Zataria multiflora* Boiss essential oil (Moradi et al., 2012), and olive oil (Pereda, Amica, & Marcovich, 2012).

Fig. 3b shows the images of the three solvents (water, formamide, and diiodomethane) drops in the three film surfaces with more marked differences between them: Ch, HWE (hydrophilic), and Oil2 (hydrophobic). The water has much less interaction with chitosan-based films than formamide or diiodomethane, confirming that the chitosan-based films nature was mainly hydrophobic.

The values of the total surface free energy and dispersive and polar components of all chitosan based films are presented in Fig. 3c. In the HWE films, the surface free energy and the dispersive component were lower in relation to Ch films, whereas the polar component was higher. The presence of some polar functional groups in the aqueous extract (OH groups of polysaccharides and polyphenols) led to a decrease of the contact angle with ultrapure water, rising the polar phase. The opposite occurs with diiodomethane, a very apolar solvent, leading to a decrease of the dispersive phase. The chitosan-based films W1, W2, and Oil1 had no differences in comparison to the control (Ch). However, the Oil2 chitosan-based film showed a higher surface free energy and dispersive phase compared with the control film, while no significant differences were observed in polar phase. These results confirm that the presence of the aqueous extract from grape pomace contributed for the increase in film hydrophilicity, while the oil incorporation increases the hydrophobicity of chitosan-based films. However, the incorporation of wax or the oil in lower concentration did not modify the films surface energy. These results are in accordance with those obtained for the solubility of chitosan films, where only the most hydrophobic film (Oil2) had a significant decrease on the solubility values when compared with the Ch film (Section 3.2).

3.4. Surface morphology analysis by atomic force microscopy

Tapping mode atomic force microscopy (AFM) was used to investigate the morphology of the surface of the chitosan film (Ch) (Fig. 4a–c), HWE (Fig. 4d–f), 0.3% of grape skin waxes (W2) (Fig. 4g–i), and 0.75% of grape seed oil (Oil2) (Fig. 4j–l).

By a macroscopic point of view, all chitosan-based films were homogenous, without cracks or macropores. However, using AFM, it was possible to verify that all films presented roughness.

Fig. 4a shows a good structural integrity of the Ch film, allowing inferring that it was robust and not easily damaged by the tip. Furthermore, it was composed of granular morphology forming fibres with an average diameter of 0.43 ± 0.08 μm arranged in the same orientation, with a hill-valley-structure surface, which is in accordance with the results described by Ghosh, Azam Ali, and Walls (2010). Fig. 4b represents the height and width ranges of the granules present in the chitosan film, based on the vertical and horizontal distances, respectively, and obtained by drawing a horizontal line over the scanned image shown in Fig. 4a. This profile of heights does not reflect the entire surface morphology of the scanned surface, but provides a representative and fairly good information of the whole sample analysed. The height profiles showed that the chitosan films had a maximum vertical distance of 7.14 ± 0.58 nm and a roughness medium square of 1.98 nm. The hill-valley-structure seems to be regular and homogeneously distributed on the surface, attributed to the distribution of uncross-linked chitosan-fibres (Ghosh et al., 2010). Fig. 4c represents the 3D view of the topography of chitosan film combining the information given by Fig. 4a and b. The general view of the scanned surface of Ch film showed well distributed hills and valleys.

The AFM analysis of HWE films showed a more homogenous surface (roughness medium square = 0.76 nm) than chitosan film (Fig. 4d–f). These films still presented the hills and valleys structure, but the maximum height was 2.63 ± 0.32 nm, more than 2.5 times lower than the control films. However, the fibre diameter was higher than Ch film (0.51 ± 0.12 μm). The polysaccharides, as well as the small portion of proteins and polyphenols of the aqueous extract, when added to the film forming solution, originate a network with the chitosan matrix, increasing the diameter of the fibres and conferring low roughness to the surface.

Fig. 4g and i display the 2D and 3D topography of chitosan-based films with incorporation of wax (W2). The W2 films have flat areas combined with large aggregates and deflection regions, leading to a roughness medium square of 6.03 nm, which is nearly 3 times higher than Ch film and ca. 8 times higher than the HWE film. These irregularities (maximum height of 15.24 ± 4.40 nm) suggest that the wax was not well dispersed in the chitosan film forming solution, probably due to the high molecular weight and hydrophobic character. However, since the wax-rich areas have a regular distribution in the film surface, it can be inferred that the waxes were well spread within the chitosan matrix. The horizontal line in Fig. 4g, traced in a flat region, allows observing the surface structure, with a maximum height of 6.8 nm, which was lower than the peak height of Ch film, but higher than HWE film, representative of a smooth surface than the Ch film but rough than the HWE film. The amount of extract could also have some influence on the morphological properties of the films, since 0.15% of hot water extract was added to the HWE film while 0.3% of wax was added to the W2 film. The presence of the fibre is less evident in the film surface when compared with the previous films.

The addition of the grape seed oil to the chitosan forming solution originated a film with a maximum peak height of 4.51 ± 1.29 nm and roughness medium square of 2.42 nm (Fig. 4j–l). The decrease of the peak height when compared with the Ch film, may indicate the existence of some weak interactions between chitosan and triacylglycerides (El-hefian, Misran, & Yahaya, 2009), such as hydrogen bonds. The oil film also showed some deflections with a regular distribution in the film surface, but these irregularities were smaller than the ones observed in the film with wax. These small aggregates could be triacylglycerides not totally dissolved in the chitosan solution due to their higher hydrophobic character.

3.5. Mechanical properties

The effect of the incorporation of grape pomace aqueous extract, wax, and oil on tensile strength, elongation at break, and Young's modulus of the films is shown in Table 2.

The chitosan film present a tensile strength (TS) of 12.61 MPa, which is similar to those reported by Vargas, Albors, Chiralt, and González-Martínez (2009). The incorporation of the higher content of wax (W2) and oil (Oil2) originated a significant decrease in the

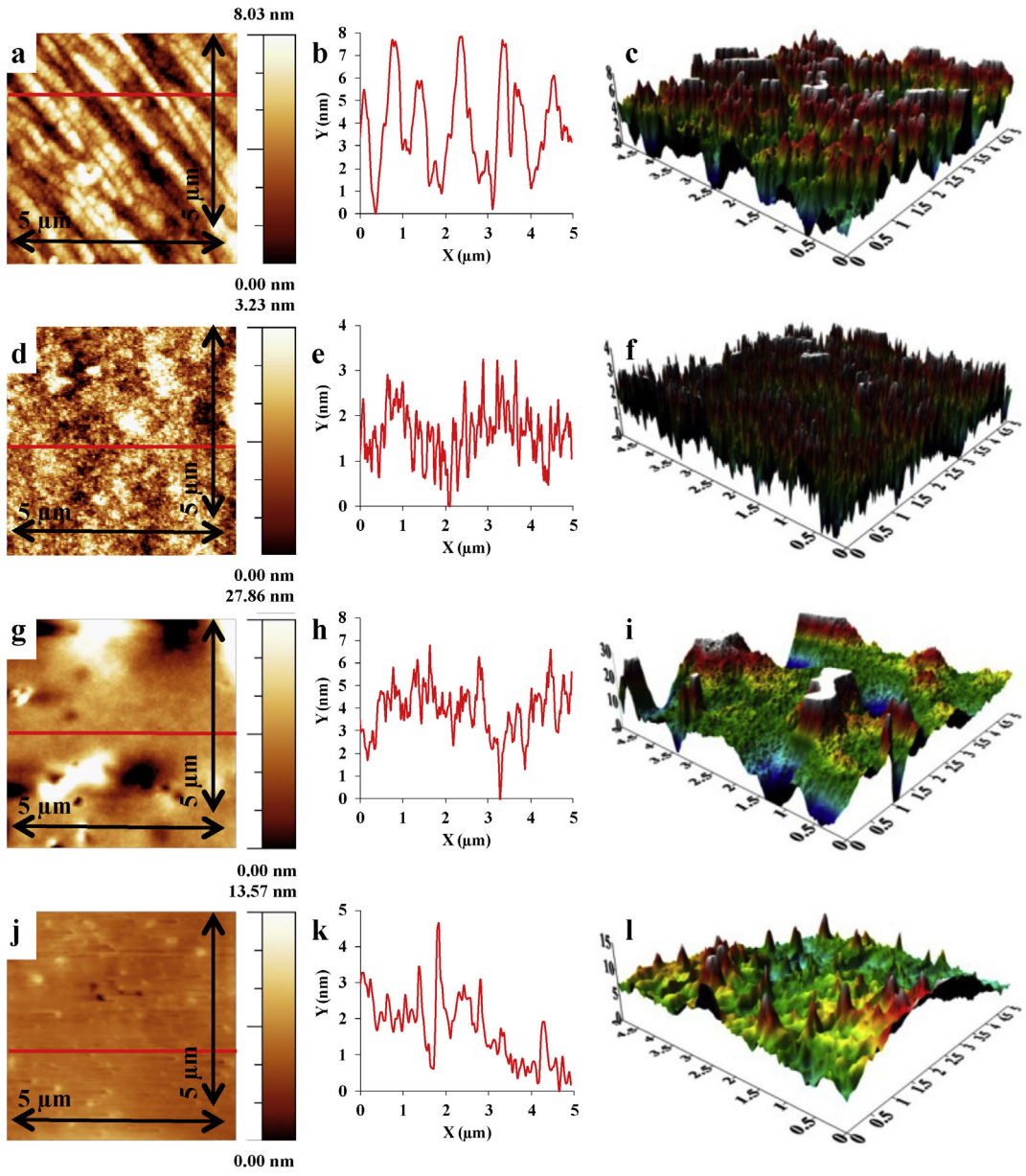

Fig. 4. Surface morphology of the chitosan-based films by AFM. 2D AFM topographic images of (a) Ch film, (d) HWE, (g) W2, and (j) Oil2 (5 × 5 µm), where the colour scale in the right side indicates the respective height values. Profile of the height values along the film in the marked area of 2D AFM topographic images of (b) Ch film, (e) HWE, (h) W2, and (k) Oil2. 3D AFM topographic images of (c) Ch film, (f) HWE, (i) W2, and (l) Oil2. (For interpretation of the references to color in this figure legend, the reader is referred to the web version of this article.)

TS of the chitosan-based films, in accordance with several other studies (Martins, Cerqueira, & Vicente, 2012; Rubilar et al., 2013; Sánchez-González et al., 2010a, 2010b).

The Elongation at break (E) of control film was 44.2%. This is a measure of the film ability to stretch prior to breakage (flexibility).

Table 2
Mechanical parameters of chitosan-based films.

	Tensile strength (MPa)	Elongation (%)	Young's modulus (MPa/%)
Ch	12.61 ± 1.59^{a}	44.24 ± 3.50^{a}	0.20 ± 0.02^{a}
HWE	13.58 ± 1.27^{a}	47.25 ± 4.11^{ab}	0.20 ± 0.02^{ab}
W1	10.99 ± 4.05^{abc}	53.48 ± 12.47^{ab}	0.13 ± 0.01^{c}
W2	9.89 ± 1.59^{b}	49.57 ± 1.79^{bc}	0.13 ± 0.02^{cd}
Oil1	12.34 ± 2.17^{ab}	41.11 ± 3.34^{ad}	0.23 ± 0.02^{b}
Oil2	6.88 ± 0.94^{c}	35.11 ± 1.96^{e}	0.16 ± 0.03^{ad}

Different superscripts letters, in each column, represent values that are significantly ($p < 0.05$) different ($n = 5$).

The value of E obtained by the different authors are very diverse, depending on the preparation conditions of the films, which could be lower ($E = 4$–28%) (Nunes et al., 2013; Rubilar et al., 2013; Sánchez-González et al., 2010b) or higher ($E = 53.85\%$) (Martins et al., 2012). No significant differences were observed in the flexibility when the grape pomace extracts were incorporated into the chitosan films, except for the W2 film that showed an increase in E (49.6%) and for the Oil2 film that showed a lower value (35.1%). These results allow to infer that the incorporation of wax led to a rise in flexibility while the oil promoted lower flexibility of the chitosan films, in agreement with previous works (Martins et al., 2012; Rubilar et al., 2013; Sánchez-González et al., 2010a, 2010b; Yoshida, Oliveira Junior, & Franco, 2009).

Young's modulus (YM), also referred as elastic modulus, is a measure of the stiffness of the film. The HWE film showed no significant differences on stiffness when compared with the control film (Ch). The incorporation of the wax into the chitosan-based

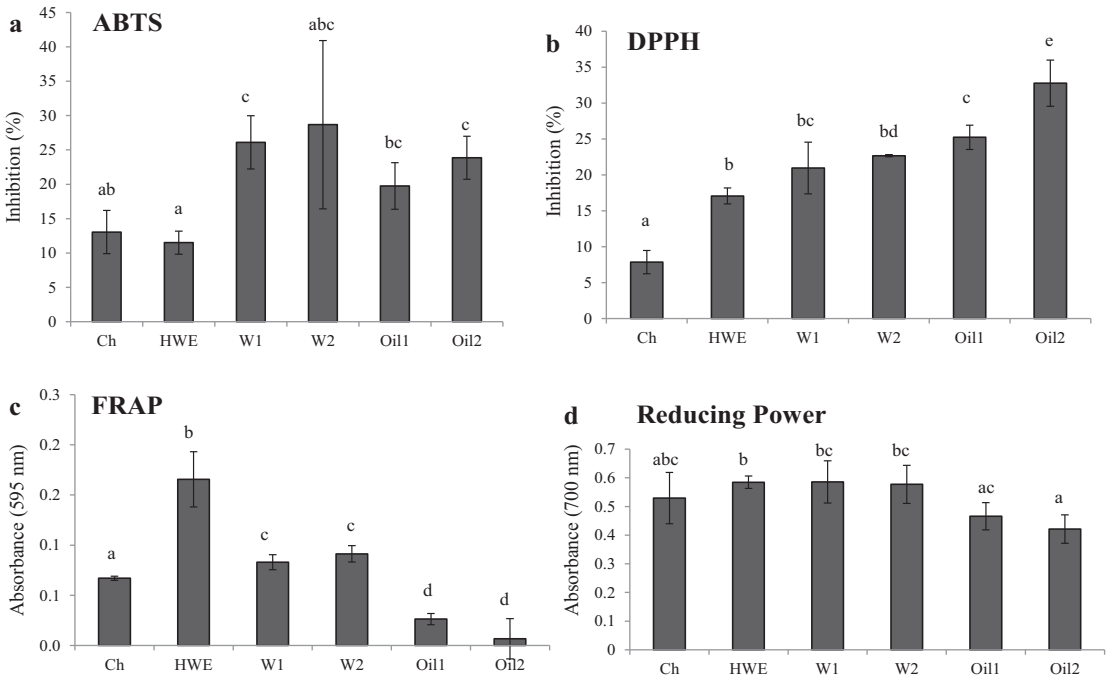

Fig. 5. Antioxidant activity of chitosan film (Ch) and chitosan-based films (HWE, W1, W2, Oil1, and Oil2) measured by: (a) ABTS, (b) DPPH, (c) FRAP, and (d) Reducing Power. Different letters represent values that are significantly ($p < 0.05$) different ($n = 3$).

films led to a decrease on YM compared to the control. The 0.3% oil incorporation in chitosan films (Oil1) led to a slight higher value of YM. However, a decrease of 30% was observed when the content of oil was two times higher (Oil2), comparing with Oil1 film stiffness. These results are in accordance with Sánchez-González et al. (2010a, 2010b), which verified that a higher percentage of bergamot and tea tree essential oil led to lower values of YM.

The addition of the HWE into the chitosan film did not change significantly its mechanical properties when compared with the Ch film. This is in accordance with the composition of the extract added (72.5% of polysaccharides) and the lower amount of HWE added (0.15%). The lower values of tensile strength, elongation, and Young' modulus for the chitosan-based films with incorporation of the higher content of waxes and oil may be related with the structural arrangement of the lipid phase into de chitosan matrix. Thus, the structural discontinuities provoked by the incorporation of the wax and oil produces a film structure with lower chain mobility and matrix cohesiveness (Martins et al., 2012), which could explain the lowest resistance to fracture, flexibility, and stiffness of these films.

3.6. Antioxidant activity

Fig. 5 shows the antioxidant activity of all chitosan-based films determined by four different methods: ABTS and DPPH, which assay the capacity of scavenge free radicals, and FRAP and Reducing Power, which evaluate the iron reducing power. The measurements of the absorbance for the different samples and antioxidant methodologies along the time, showing the zones of linearity for each one, are given as Supplementary material (Fig. S2).

The antioxidant activity of the control films represented 13% of inhibition when measured by ABTS method (Fig. 5a). This activity can be attributed to the capacity of chitosan amino groups to react with free radicals, originating stable macromolecular radicals and protonated ammonium (NH_3^+) groups (Xie, Xu, & Liu, 2001). It was not observed significant differences between the control and the HWE film. However, the incorporation in the chitosan films of grape skin wax in a concentration of 0.15% (W1) and grape seed oil in a concentration of 0.75% (Oil2) affected positively their antioxidant properties, with an increase of 100% and 83%, respectively, when compared with the control films. The incorporation in chitosan films of all grape pomace extracts led to a higher antioxidant activity by DPPH method (Fig. 5b). These results allowed to conclude that the incorporation of the polysaccharides-rich extract, waxes, and oil into chitosan-based films contributed to enhance their scavenge free radical capacity.

The antioxidant activity determined by FRAP method is shown in Fig. 5c. FRAP test is based on the ability of antioxidants to reduce ferric tripyridyltriazine complex (Fe(III)-TPTZ) to the blue ferrous complex Fe(II)-TPTZ. The chitosan film with aqueous extract (HWE) exhibited an antioxidant activity 2.5 times higher when compared to the control. The W1 and W2 also demonstrated a higher antioxidant activity (24 and 36%, respectively) than control, whereas the Oil1 and Oil2 showed a decrease. On the contrary, no significant differences in antioxidant activities were observed between the control (Ch) and all chitosan-based film using the reducing power method (Fig. 5d), which is based on ion electron-transfer reactions. The only significant difference was the decreasing of antioxidant activity of Oil1 in 20% and Oil2 in 28% compared with the HWE chitosan-based film.

Considering all the antioxidant methods used, it is possible to verify that the antioxidant capacity of the films with the different grape pomace extracts, when compared to the Ch films, varies with the method used. If the method uses an organic solvent, as in ABTS and DPPH, which have been prepared in ethanol, the most hydrophobic films such as W1, W2, Oil1, and mainly Oil2 showed higher antioxidant activities when compared with the control for the same assay. Otherwise, in an aqueous medium, as in FRAP and Reducing Power methods, the most hydrophilic films (HWE) revealed the highest antioxidant activity when compared with the respective control.

Besides the differences between the methodologies to determine the antioxidant activity, all the chitosan based films containing the incorporated grape pomace extracts showed higher antioxidant capacities than the respective control films. These

statements are based on the presented results as well as on previous results obtained with the chitosan films used in the preliminary experiments (Supplementary material Fig. S3).

The degree of antioxidant capacity of edible film was generally proportional to the amount of the antioxidant additives added. The aqueous extract exhibited an antioxidant activity of 42 mg/L of Trolox equivalents (ABTS assay) and the grape seed oil had an antioxidant activity of 0.24 mM tocopherol equivalents (DPPH assay). Their inclusion in the films confers them antioxidant activity. The results obtained are in line with other studies with chitosan-based films incorporated with alfa-tocopherol (Martins et al., 2012), grape seed extract, an essential oil of *Z. multiflora* Boiss (Moradi et al., 2012), and green tea extract (Siripatrawan & Harte, 2010).

4. Conclusion

The results of the present work showed that the incorporation in chitosan film of grape pomace extracts, which comprised an aqueous extract (mainly polysaccharides), a grape skin wax extract, and grape seed oil, allowed the development of films with modulation of their properties. Chitosan-based films with the incorporation of the aqueous extract were the most hydrophilic and smoothest film, revealing enhanced antioxidant properties without modification of their water solubility and mechanical properties. The incorporation of wax in the chitosan solution produced a film more heterogeneous and rough but allowed the improvement of the antioxidant properties with no significant changes in solubility. The wax also contributed for the increase of the films flexibility and decrease of stiffness. The chitosan-based films with oil were the most hydrophobic ones, presenting higher antioxidant activities and a slight lower solubility in water. The surface morphology showed that the Oil2 film had a roughness similar to the Ch film. These oil films revealed slight different mechanical properties, such as lower resistance to fracture, flexibility, and stiffness, mainly for the film with the incorporation of the higher proportion of oil. Therefore, all these films can be a promising alternative to synthetic materials and as a vehicle for functional compounds, contributing to biological applications, including food shelf-life extension. For that, the dissolution of the chitosan in acetic acid should be stoichiometric in order to avoid the presence of excess of acetic acid which could substantially alter the characteristics of the films. Otherwise, other weak acids could be also used, such as formic and lactic acids, to dissolve the chitosan avoiding the presence of acetic acid in the films.

Acknowledgments

Thanks are due to Fundação para a Ciência e a Tecnologia (FCT, Portugal), European Union, QREN, FEDER, and COMPETE for funding the QOPNA research unit (project PEst-C/QUI/UI0062/2013; FCOMP-01-0124-FEDER-037296), CICECO (Pest-C/CTM/LA0011/2013; FCOMP-01-0124-FEDER-037271), and FCT project (PTDC/AGR-ALI/101251/2008). C. Nunes, A. Castro and P. Ferreira thank FCT for the Post-Doctoral fellowship SFRH/BPD/46584/2008, Doctoral fellowship SFRH/BD/67121/2009, and research position IF/00327/2013, respectively. The authors also thank Dão Sul—Sociedade Vitivinícola S.A (Carregal do Sal, Portugal) for providing the grape pomace.

Appendix A. Supplementary data

Supplementary material related to this article can be found, in the online version, at http://dx.doi.org/10.1016/j.carbpol.2014.07.032.

References

Ainsworth, E. A., & Gillespie, K. M. (2007). Estimation of total phenolic content and other oxidation substrates in plant tissues using Folin–Ciocalteu reagent. *Nature Protocols*, *2*, 875–877.

Aranaz, I., Mengibar, M., Harris, R., Panos, I., Miralles, B., Acosta, N., & Gemma, G. (2009). Functional characterization of chitin and chitosan. *Current Chemical Biology*, *3*, 203–230.

Aued-Pimentel, S., Lago, J. H. G., Chaves, M. H., & Kumagai, E. E. (2004). Evaluation of a methylation procedure to determine cyclopropenoids fatty acids from Sterculia striata St. Hil. Et Nauds seed oil. *Journal of Chromatography A*, *1054*, 235–239.

Benzie, I. F. F., & Strain, J. J. (1996). The ferric reducing ability of plasma (FRAP) as a measure of "antioxidant power": The FRAP assay. *Analytical Biochemistry*, *239*, 70–76.

Blumenkrantz, N., & Asboe-Hansen, G. (1973). New method for quantitative determination of uronic acids. *Analytical Biochemistry*, *54*, 484–489.

Bourbon, A. I., Pinheiro, A. C., Cerqueira, M. A., Rocha, C. M. R., Avides, M. C., Quintas, M. A. C., & Vicente, A. A. (2011). Physico-chemical characterization of chitosan-based edible films incorporating bioactive compounds of different molecular weight. *Journal of Food Engineering*, *106*, 111–118.

Busilacchi, A., Gigante, A., Mattioli-Belmonte, M., Manzotti, S., & Muzzarelli, R. A. A. (2013). Chitosan stabilizes platelet growth factors and modulates stem cell differentiation toward tissue regeneration. *Carbohydrate Polymers*, *98*, 665–676.

Chen, A. S., Taguchi, T., Sakai, K., Kikuchi, K., Wang, M. W., & Miwa, I. (2003). Antioxidant activities of chitobiose and chitotriose. *Biological & Pharmaceutical Bulletin*, *26*, 1326–1330.

Chien, P.-J., Sheu, F., Huang, W.-T., & Su, M.-S. (2007). Effect of molecular weight of chitosans on their antioxidative activities in apple juice. *Food Chemistry*, *102*, 1192–1198.

Coimbra, M. A., Waldron, K. W., & Selvendran, R. R. (1994). Isolation and characterisation of cell wall polymers from olive pulp (*Olea europaea* L.). *Carbohydrate Research*, *252*, 245–262.

Deng, Q., Penner, M. H., & Zhao, Y. (2011). Chemical composition of dietary fiber and polyphenols of five different varieties of wine grape pomace skins. *Food Research International*, *44*, 2712–2720.

Deng, Q., & Zhao, Y. (2011). Physicochemical, nutritional, and antimicrobial properties of wine grape (cv. Merlot) pomace extract-based films. *Journal of Food Science*, *76*, 309–317.

Dutta, P. K., Tripathi, S., Mehrotra, G. K., & Dutta, J. (2009). Perspectives for chitosan based antimicrobial films in food applications. *Food Chemistry*, *114*, 1173–1182.

El-hefian, E. A., Misran, M., & Yahaya, A. H. (2009). Surface investigation of chitosan film with fatty acid monolayers. *Maejo International Journal of Science and Technology*, *3*, 277–286.

Fernandes, S. C. M. (2010). *Novel materials based on chitosan, its derivatives and cellulose fibres*. Aveiro: University of Aveiro.

Ghosh, A., Azam Ali, M., & Walls, R. (2010). Modification of microstructural morphology and physical performance of chitosan films. *International Journal of Biological Macromolecules*, *46*, 179–186.

Hosseini, M. H., Razavi, S. H., & Mousavi, M. A. (2009). Antimicrobial, physical and mechanical properties of chitosan-based films incorporated with thyme, clove and cinnamon essential oils. *Journal of Food Processing and Preservation*, *33*, 727–743.

Huang, D. J., Ou, B. X., & Prior, R. L. (2005). The chemistry behind antioxidant capacity assays. *Journal of Agricultural and Food Chemistry*, *53*, 1841–1856.

Kong, M., Chen, X. G., Xing, K., & Park, H. J. (2010). Antimicrobial properties of chitosan and mode of action: A state of the art review. *International Journal of Food Microbiology*, *144*, 51–63.

Krohn, R. I. (2001). The colorimetric detection and quantitation of total protein. In R. E. Wrolstad, T. E. Acree, E. A. Decker, M. H. Penner, D. S. Reid, S. J. Schwartz, C. F. Shoemaker, D. M. Smith, & P. Sporns (Eds.), *Current Protocols in Food Analytical Chemistry (B1.1.1-B1.1.28)*. New York: Wiley.

Kumar, M. R., Muzzarelli, R. A., Muzzarelli, C., Sashiwa, H., & Domb, A. (2004). Chitosan chemistry and pharmaceutical perspectives. *Chemical Reviews*, *104*, 6017–6084.

Lagaron, J. M., Fernandez-Saiz, P., & Ocio, M. J. (2007). Using ATR-FTIR spectroscopy to design active antimicrobial food packaging structures based on high molecular weight chitosan polysaccharide. *Journal of Agricultural and Food Chemistry*, *55*, 2554–2562.

Leceta, I., Guerrero, P., Ibarburu, I., Dueñas, M. T., & de la Caba, K. (2013). Characterization and antimicrobial analysis of chitosan-based films. *Journal of Food Engineering*, *116*, 889–899.

Martins, J. T., Cerqueira, M. A., & Vicente, A. A. (2012). Influence of α-tocopherol on physicochemical properties of chitosan-based films. *Food Hydrocolloids*, *27*, 220–227.

Moradi, M., Tajik, H., Razavi Rohani, S. M., Oromiehie, A. R., Malekinejad, H., Aliakbarlu, J., & Hadian, M. (2012). Characterization of antioxidant chitosan film incorporated with *Zataria multiflora* Boiss essential oil and grape seed extract. *LWT—Food Science and Technology*, *46*, 477–484.

Nunes, C., Maricato, É., Cunha, Â., Nunes, A., Silva, J. A. L., & Coimbra, M. A. d. (2013). Chitosan–caffeic acid–genipin films presenting enhanced antioxidant activity and stability in acidic media. *Carbohydrate Polymers*, *91*, 236–243.

Ojagh, S. M., Rezaei, M., Razavi, S. H., & Hosseini, S. M. H. (2010). Development and evaluation of a novel biodegradable film made from chitosan and cinnamon essential oil with low affinity toward water. *Food Chemistry*, *122*, 161–166.

Pereda, M., Amica, G., & Marcovich, N. E. (2012). Development and characterization of edible chitosan/olive oil emulsion films. *Carbohydrate Polymers*, *87*, 1318–1325.

Rhim, J., Weller, C., & Ham, K. (1998). Characteristics of chitosan films as affected by the type of solvent acid. *Food Science and Biotechnology*, *7*, 263–268.

Rubilar, J. F., Cruz, R. M. S., Silva, H. D., Vicente, A. A., Khmelinskii, I., & Vieira, M. C. (2013). Physico-mechanical properties of chitosan films with carvacrol and grape seed extract. *Journal of Food Engineering*, *115*, 466–474.

Sánchez-González, L., Cháfer, M., Chiralt, A., & González-Martínez, C. (2010). Physical properties of edible chitosan films containing bergamot essential oil and their inhibitory action on *Penicillium italicum*. *Carbohydrate Polymers*, *82*, 277–283.

Sánchez-González, L., González-Martínez, C., Chiralt, A., & Cháfer, M. (2010). Physical and antimicrobial properties of chitosan–tea tree essential oil composite films. *Journal of Food Engineering*, *98*, 443–452.

Schieber, A., Stintzing, F. C., & Carle, R. (2001). By-products of plant food processing as a source of functional compounds—recent developments. *Trends in Food Science & Technology*, *12*, 401–413.

Shahidi, F., Arachchi, J. K. V., & Jeon, Y. J. (1999). Food applications of chitin and chitosans. *Trends in Food Science & Technology*, *10*, 37–51.

Silva, S. S., Goodfellow, B. J., Benesch, J., Rocha, J., Mano, J. F., & Reis, R. L. (2007). Morphology and miscibility of chitosan/soy protein blended membranes. *Carbohydrate Polymers*, *70*, 25–31.

Siripatrawan, U., & Harte, B. R. (2010). Physical properties and antioxidant activity of an active film from chitosan incorporated with green tea extract. *Food Hydrocolloids*, *24*, 770–775.

Soares, N. M., Mendes, T. S., & Vicente, A. A. (2013). Effect of chitosan-based solutions applied as edible coatings and water glazing on frozen salmon preservation—A pilot-scale study. *Journal of Food Engineering*, *119*, 316–323.

Srinivasa, P. C., Ramesh, M. N., & Tharanathan, R. N. (2007). Effect of plasticizers and fatty acids on mechanical and permeability characteristics of chitosan films. *Food Hydrocolloids*, *21*, 1113–1122.

Tharanathan, R. N. (2003). Biodegradable films and composite coatings: Past, present and future. *Trends in Food Science & Technology*, *14*, 71–78.

Vargas, M., Albors, A., Chiralt, A., & González-Martínez, C. (2009). Characterization of chitosan–oleic acid composite films. *Food Hydrocolloids*, *23*, 536–547.

Xie, W., Xu, P., & Liu, Q. (2001). Antioxidant activity of water-soluble chitosan derivatives. *Bioorganic & Medicinal Chemistry Letters*, *11*, 1699–1701.

Yoshida, C. M. P., Oliveira Junior, E. N., & Franco, T. T. (2009). Chitosan tailor-made films: The effects of additives on barrier and mechanical properties. *Packaging Technology and Science*, *22*, 161–170.

Zhang, Y., Yang, Y., Tang, K., Hu, X., & Zou, G. (2008). Physicochemical characterization and antioxidant activity of quercetin-loaded chitosan nanoparticles. *Journal of Applied Polymer Science*, *107*, 891–897.